Adhesion Strength of TiN Stacked TiO_2 Film Correlated with Contact Angle, Critical Load, and XPS Spectra

Shankar PARAJULEE, Masahiro HAYAKAWA and Shunjiro IKEZAWA

Department of Electrical and Electronic Engineering, Graduate School of Engineering, Chubu University, Kasugai, Aichi 487–8501, Japan

(Received 21 July 2009 / Accepted 23 October 2009)

In order to coat TiO_2 and TiN/TiO_2 films on glass over a large surface area for industrial application, plasma gun and magnetron sputtering processes were used. Also, nitrogen radicals were synthesized on the surface via the atmospheric plasma process. Hydrophilic characteristics were studied via water contact angle. Film adherence was tested via single stylus scratch tester. We also compared the XPS spectra between the nitrogen-synthesized and non-synthesized film and obtained the Ti2p peak shift towards the higher energy level proportional to film adherence. For photocatalytic film durability, the relationship best described, "the higher the critical load, the lower the contact angle, and the higher the binding energy" has become a unique interrelationship among the scratch tester, contact angle, and XPS spectra.

Keywords: single stylus scratch tester, contact angle, XPS spectra, nitrogen incorporation

DOI: 10.1585/pfr.4.055

1. Introduction

Thin film titania (TiO_2) is a versatile material and has been the subject of sustained research interest. The major challenge to the lifetime of TiO_2 thin film is the adhesive strength dependency on deposition condition. Many proposed methods for testing adhesion have been reviewed [1, 2]. One major experimental difficulty in thin film coating adhesion testing is that of creating a mechanical linkage to the coated film in order to elucidate substrate adherence. The scratch test solves this linkage problem and has often been used to study adhesion [3–6]. Previously, the lifetime of the TiO_2 thin film was popularly analyzed by contact angle measurement [7]. However, contact angle measurement analysis cannot describe the mechanical linkage of the coating material and substrate.

In this study, we prepared TiO_2 film using the magnetron sputtering method, TiN film by plasma gun, and nitrogen radicals by atmospheric plasma jet. Film adhesive character was then analyzed using a single stylus diamond scratch tester. The scratch test consists of deforming the coated surface by indentation under the load of a moving diamond blade. The applied load is increased in a stepwise fashion or continuously until the coated film becomes unable to follow the deformation of the substrate. The diamond stylus is drawn under a selected load across the coating surface. Adhesive failure and stylus acoustic signal induction are then recorded via audio microphone. We found that the onset of determinant acoustic signals strongly depends upon the method of TiO_2 thin film synthesis (i.e., nitrogen-incorporated TiO_2 film possesses more adhesive strength).

We used water contact angle to investigate film wettability and X-ray photoelectron spectroscopy to perform a Ti2p peak shift comparative analysis in accordance with TiN stacked and non-stacked film adherences.

2. Experimental Setup

2.1 Sample preparation

Four different thin films of uniform thickness (50 nm) were deposited on the glass surface under vacuum and without vacuum (atmospheric pressure). The details of each sample are as follows.

i. Glass/TiO_2 was deposited by pulse DC magnetron sputtering method in a meter-sized plasma reactor.
ii. Glass/TiN/TiO_2 was deposited by plasma gun for TiN and sputtering technique for TiO_2.
iii. Glass/TiO_2/N_2 jet (TiON) was prepared by atmospheric pressure plasma jet-mounting the thin film of Sample (i) by N_2 plasma jet.
iv. Glass/TiN/TiO_2/N_2 jet (TiON) was prepared by atmospheric pressure plasma jet mounting the thin film of Sample (ii) by N_2 plasma jet.

2.2 Instrumentation

2.2.1 Plasma gun for TiN coating

A buffer layer of TiN film was deposited by Ti-source metal evaporation in a meter-sized PVD. We have further developed the plasma gun (~150 V, ~500 A) for marketing at a smaller size (~100 V, ~100 A) and more popular use. The gun was laterally mounted to a large diameter reactor

author's e-mail: Shankarparajulee94@hotmail.com

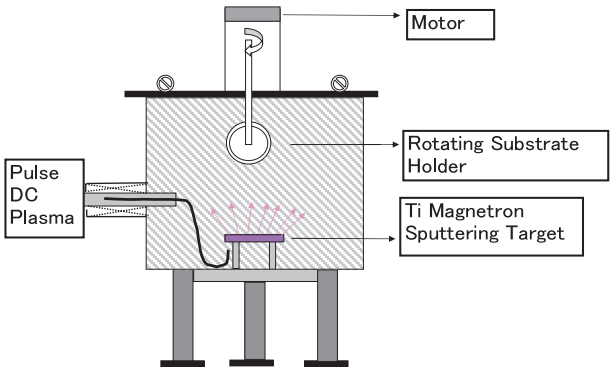

Fig. 1 Schematic diagram of magnetron sputtering apparatus.

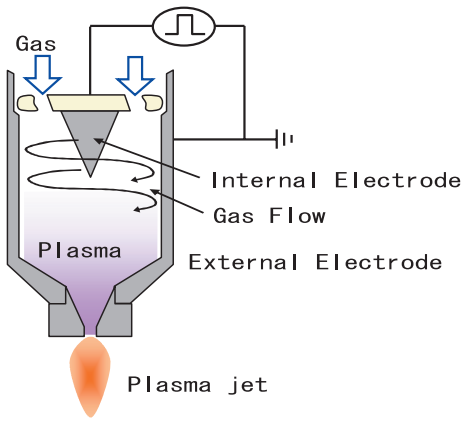

Fig. 2 Schematic diagram of atmospheric pressure plasma jet device.

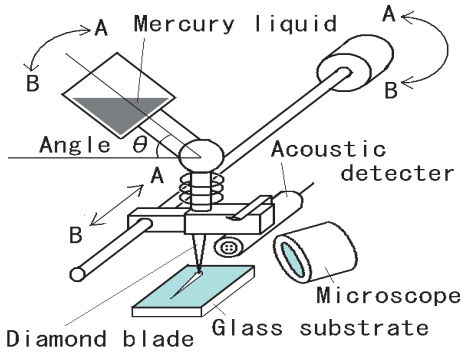

Fig. 3 Schematic diagram of single stylus diamond scratch tester.

(1.2 m). Ti atoms from molten Ti residing in an anode pot were vaporized in N_2 plasma. The parameters of the process were as follows: N_2 gas at 5 sccm, Ar gas at 15 sccm, gas pressure at 1 mTorr, gun voltage at 90 V and current at 60 A. Coating time was 30 sec, film color was translucent with film thickness ~10 nm.

2.2.2 Magnetron sputtering for TiO_2 coating

We have developed a large area magnetron sputtering apparatus with a 37 cm^2 Ti target plate source, as is shown in Fig. 1. The target was placed at the bottom of a large diameter reactor (1.2 m). A reactive plasma generator (RPG-100) was used as the plasma source. Ti atoms from the target source were then evaporated in oxygen plasma. The sputtering process was used regularly for TiO_2 film coating. The process parameters were as follows: O_2 gas flow at 15 sccm, Ar gas flow at 15 sccm, gas pressure at 34 mTorr, sputtering power source at 1 kW, 100 kHz, pulse duty rate 50%, coating time 10 minutes, film color: transparent, film thickness ~10 nm. The deposition time was adjusted to achieve the desired 50 nm film thickness.

2.2.3 Nitrogen spray by atmospheric pressure plasma Jet

An atmospheric plasma jet schematic is depicted in Fig. 2. Prepared plasma in the coaxial electrode region is ejected in jet form with a 480°C flame temperature at 0.5 cm distance from the nozzle edge. The outer and inner nozzle diameters are 25 mm and 4 mm, respectively. The operational conditions are listed as follows: electrical discharge source frequency 16 kHz, electrical power 1.5 kW, and N_2 gas flow 30 L/min. Operation continued for 1 minute to embed nitrogen on the film without changing film thickness significantly.

2.2.4 Scratch test for adherence strength

The scratch test consists of deforming the coated surface by indentation under the load of a moving diamond blade (Fig. 3). The load under which coating detachment occurs is considered as an adhesion measure. One major problem associated with the scratch test is the fact that the relationship between the measured critical load and the actual cohesion strength is not yet clear. Among the various definitions proposed, Perry [8] introduced the concept of coating loss onset as a factor of critical load. In this concept, the minimum load at which the coating surface incurs damage is considered the critical load. For our adhesion studies, the scratch test was performed under standard conditions (diamond tip diameter 0.4 mm; scratching speed dx/dt = 10 mm/min; and loading adjusted in angular movement). Thus critical load (L_c) = $9.8(0.15 + W \sin\theta)$, where W = 1.5 kg is a constant mercury load and 0.15 kg is for θ = 0°, and is calculated for every corresponding θ. The details of the developed scratch tester are shown in Fig. 3.

2.2.5 Water contact angle meter

The contact angle is the angle at which a liquid/vapor interface meets a solid surface. The water contact angle on the glass substrate is measured via the sessile drop method using a contact angle meter FACE CAD [9,10]. A tungsten

lamp (visible light) and a fluorescent lamp (UV - visible light) (25 μW/cm^2, 17 K lux) serve as irradiation sources. The water contact angles are measured at 0, 10, 20, and 30 minutes beyond light source activation. Also, contact angle recovery is observed for 20 min beyond irradiation source deactivation.

3. Results and Discussions

The TiN-stacked nitrogen-incorporated TiO_2 films aim to increase film adherence. Previous studies [8, 11–15] indicate that critical load increased linearly with substrate hardness. Also, critical load increased with coating thickness [16]. Keeping these facts in mind, we have studied four film types in a common glass substrate and in uniform thickness. In Fig. 4, the film flaking distance L (the angle θ) is measured via acoustic detector, measuring the first surface scratch signal acoustic emission [8]. The adhesion strengths (critical loads) L_c were calculated and are visible in Fig. 5. As is shown in Figs. 4 and 5, it was found that the required critical load for scratch onset is approximately 6 N in TiN-interfaced TiO_2 film, whereas it was only 5 N in the TiO_2 film. This result is vexing [8, 11–16] because the film thickness is constant and the glass substrate is identical. TiN, with its high bonding capability, should have provided the adhesive interface to increase film adherence. Moreover, there was no difference in film adherence due to nitrogen incorporation. Due to TiO_2 bond flexibility, atomic (nascent) nitrogen in the plasma jet may only be employed to prepare an intimate composite layer (TiON) and to increase the photocatalytic property.

Figure 6 presents the water contact angles of the untreated glass, TiO_2-treated, and TiON-treated glass substrate. The contact angle decreases in the first step at TiO_2 and TiON coating from ~55 degrees to ~4 degrees without irradiation. Additionally, following tungsten lamp and fluorescent lamp irradiation, the contact angle decreases further, 2 to 3 degrees. However, as the light deactivates after 10 min, the contact angle continues increasing up to 12 degrees with the time delay of 20 minutes to light removal. Due to this characteristic of slight contact angle decrease with light irradiation and contact angle recovery with irradiation removal, it can be concluded that the film possesses photocatalytic properties [17].

Ti2p peak XPS spectra effects due to TiN stacking and on-film nitrogen synthesis are depicted in Fig. 7. Figure 7 also reveals that there was a slight peak shift towards a higher energy level as TiN proceeded to stack with TiO_2, or as film adhesion increased. Examining the spectrum, two main Ti2p doublet peaks are visible, where the more intense Ti2$p_{3/2}$ peak at 459.1 eV shifts by 0.42 eV, with the known value 458.68 eV for pure TiO_2. At 460 eV, a shift of 1.32 eV occurs for the TiN-stacked TiO_2 with N_2 jet treatment. Due to titanium atomic concentration dependence on the multilayered film [18, 19], the Ti2p peak might have increased where higher binding energy was present. This

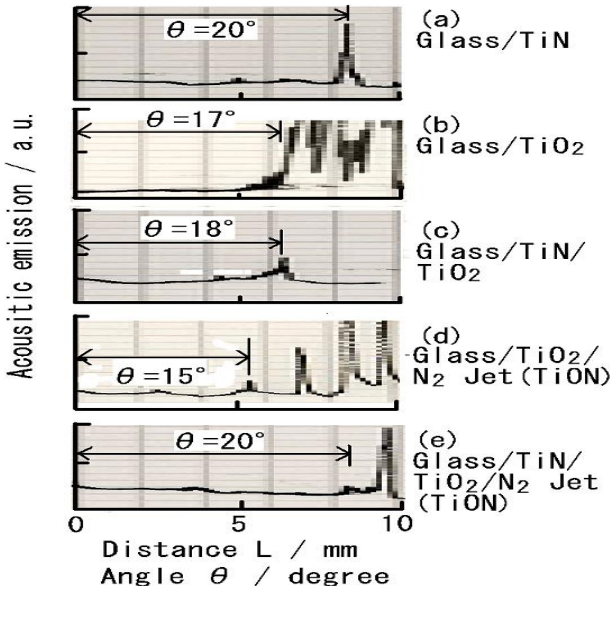

Fig. 4 Acoustic emissions during thin film flaking.

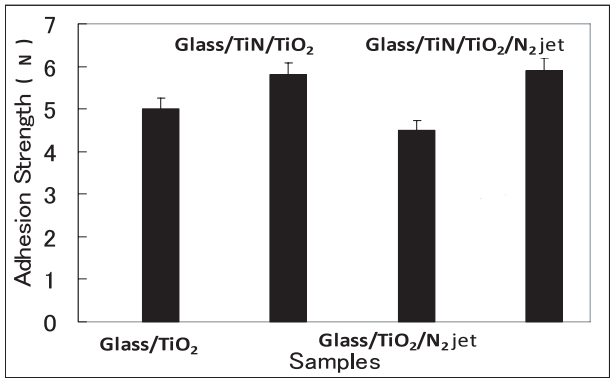

Fig. 5 Comparison of critical load for an average of 4 scratches.

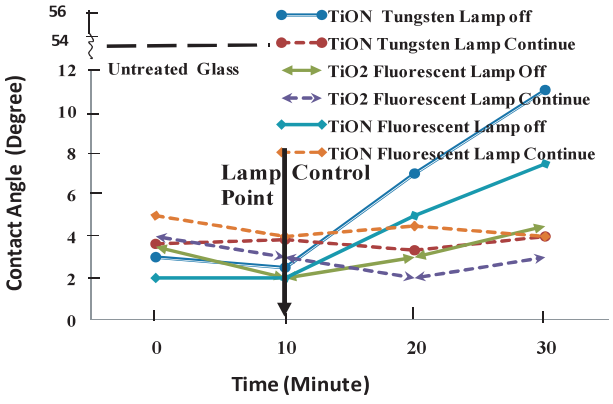

Fig. 6 Water contact angles of Glass/TiN/TiO_2/N_2 (TiON) and Glass/TiN/TiO_2 (TiO_2) irradiated by tungsten lamp and fluorescent lamp. Irradiation cut off after 10 min is indicated by "lamp off."

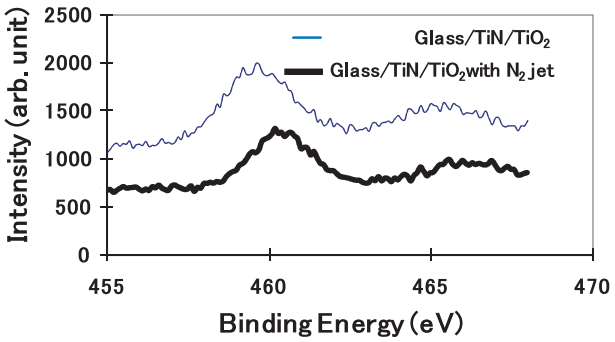

Fig. 7 XPS spectra of Glass/TiN/TiO_2//N_2 (TiON) and Glass/TiN/TiO_2 (TiO_2) film.

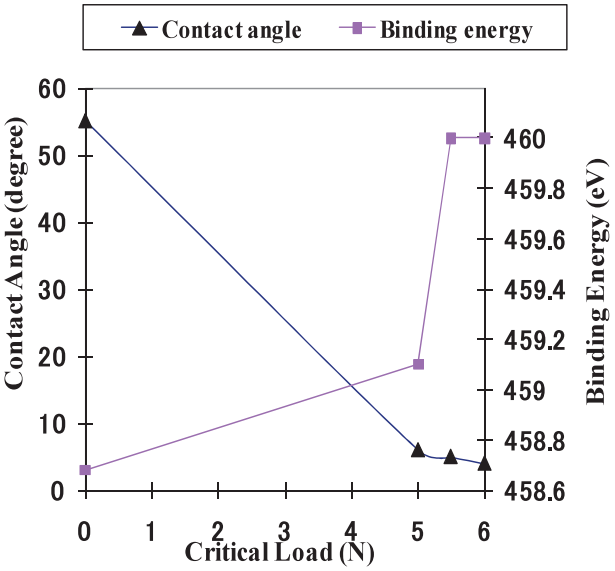

Fig. 8 Relationship among contact angle, critical load and binding energy for TiON film.

shift in the Ti2p binding energy indicates that the TiN and TiO_2 are forming an intimate mixture, so that the electron states of the composite are not simply described by separate phases consisting of the pure materials. Also, peak shift by 1.32 eV in sample (iv) indicates that TiO_2 treated by N_2 plasma jet results in the formation of an intimate mixture of TiON, producing a photocatalytic film (Fig. 6). Regardless of the critical XPS analysis for film surface chemistry, we have achieved a simple ideology (Fig. 8), described best as: "the higher the adhesion strength, the lower the contact angle, and the higher the binding energy."

4. Conclusions

TiN/TiO_2 thin-film adhesion strengths following glass substrate deposition were compared according to the critical load measured in the scratch test. The critical load resulting in film delamination or in delamination propagation was determined accurately via acoustic emission during diamond blade loading. It was discovered that TiO_2 film adhesive strength increased from 5 N to 6 N when TiN was sandwiched using the same substrate. Also, while TiON film failed to demonstrate a distinct alteration in film hardness, it succeeded in altering its photocatalytic properties. While water contact angle was found to decrease almost uniformly for nitrogen-synthesized and non-synthesized film, the contact angle demonstrated remarkable recovery in nitrogen-synthesized film, confirming photocatalysis in nitrogen-synthesized film. There was a considerable discrepancy between the XPS Ti2p peak position value of TiN-stacked TiO_2 film and that of the well-established value for TiO_2 film. Comparison with previous literature data fostered our assumption that nitrogen suffusion in TiO_2 film helped to vary the Ti2p film content, leading to the formation of an intimate composite layer. Nonetheless, having analyzed contact angle, adhesion strength, and XPS spectra, each independently, their joint correlation has been evaluated.

Acknowledgments

This work was supported in part by grants from the Gonbru scholarship of Nagoya University, the Knowledge Cluster and the special fund of Chubu University.

[1] C. Weaver, Chem. Ind. (NY) **1**, 370 (1965).
[2] B.N. Chapman, J. Vac. Sci. Technol. **11**, 106 (1974).
[3] O.S. Heavens, J. Phys. Radium. **11**, 355 (1950).
[4] P. Benjamin and C. Weaver, Proc. R. Soc. London, Ser. A **254**, 163 (1960).
[5] P. Benjamin and C. Weaver, Proc. R. Soc. London, Ser. A **274**, 267 (1963).
[6] C. Weaver, J. Vac. Sci. Technol. **12**, 18 (1975).
[7] H. Homyara and S. Ikezawa, Recent Research Developments in Vac. Sci. Technol. **4**, 61 (2003).
[8] A.J. Perry, Thin Solid Films **107**, 167 (1983).
[9] S. Parajulee and S. Ikezawa, Industrial Application of Plasma Process **1**, 17 (2008).
[10] S. Parajulee and S. Ikezawa, Industrial Application of Plasma Process **1**, 27 (2008).
[11] P. Asteinman, P. Laeng and H.E. Hintermann, Mater. Tech. **13**, 85 (1985).
[12] P. Laeng and P.A. Steinmann, Proceeding of the 8th International Conference on Chemical Vapor Deposition, Paris, 1981 (Electro-chemical Society, Pennington, N.J., 1981) p.723.
[13] B. Hammer, P. Laeng and P.A. Steinman, Thin Solid Films **96**, 45 (1982).
[14] K.L. Chopra, in *Thin Film Phenomena* (McGraw-Hill, New York, 1969) p.313.
[15] A. Pan and J.E. Greene, Thin Solid Films **97**, 79 (1982).
[16] P.A. Steinmann and H.E. Hintermann, J. Vac. Sci. Technol. **3**, 323 (1985).
[17] M. Takeuchi, S. Doshi and T. Eura, J. Phy. Chem. B **107**, 14278 (2003).
[18] R.P. Netterfield, P.J. Martin, *et al.*, J. Appl. Phys. **66**, 1805 (1989).
[19] M. Andrulevicius and S. Tamulevicius, Material Science **14**, 8 (2008).